THE UNIVERSITY OF

WARWICK

In-Situ Synchrotron Diffraction of the Electrochemical Reduction Pathway of TiO_2

R. Bhagat[a], D. Dye[b], S. L. Raghunathan[b], R. J. Talling[b], D. Inman[b], B. K. Jackson[b], K. K. Rao[c], and R. J. Dashwood[a]

[a] *University of Warwick, Coventry, CV4 7AL, UK*
[b] *Imperial College, London, SW7 2AZ, UK*
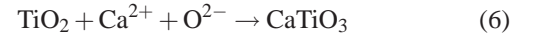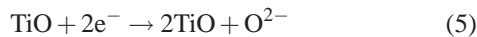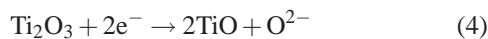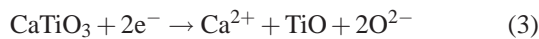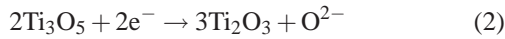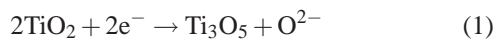[c] *Metalysis, Rotherham, S63 5DB, UK*

Despite over ten years of research into the low-cost electrowinning of titanium direct from the oxide, the reduction sequence of TiO_2 pellets in molten $CaCl_2$ has been the subject of debate, particularly as the reduction pathway has been inferred from ex-situ studies. Here, for the first time white beam synchrotron X-ray diffraction is used to characterize the phases that form, in-situ during reduction and with $\sim 100\,\mu m$ spatial resolution. It is found that TiO_2 becomes sub-stoichiometric very early in reduction facilitating the ionic conduction of oxygen ions, that $CaTiO_3$ persists to nearly the end of the process and that, finally, CaO forms just before completion of the process. The method is quite generally applicable to the in-situ study of industrial chemical processes. Implications for the industrial scale-up of this method for the low-cost production of titanium are drawn.

I. INTRODUCTION

The FFC Cambridge process is an electrochemical method by which metal oxides are reduced to metal using a molten chloride flux [1]. The process is thought to have the potential to lead to a step change in the cost of extraction of several metal alloy systems, including titanium. Currently the most widely used method for extracting titanium from rutile is the Kroll process [2].

The FFC Cambridge reduction of TiO_2 involves the progressive reduction and deoxidation of a porous TiO_2 pellet cathode in a molten halide salt. At the cathode the titanium oxide is reduced to titanium and the oxide ions dissolve into the calcium chloride. These oxide ions migrate to a carbon anode where they form carbon dioxide and carbon monoxide. The reduction pathway for this process has been studied using a combination of pellet reductions [3], metal-cavity electrode [4] and thin-film experimentation [5].

Previous work by the present authors has focussed on the reduction of TiO_2 using thin films [5] and metal-cavity electrodes [4]. Using cyclic voltammetry, these studies identified several electrochemical events taking place during reduction. These electrochemical events C4, C3, C2', C2 and C1 were identified as reactions 1 to 6 respectively, using *ex-situ* X-ray diffraction (XRD) analysis of the thin-films removed after each reduction event. Despite being observed in XRD, the formation of $CaTiO_3$ was not observed on the voltammograms. As such it was believed to form via a chemical reaction [6].

$$2TiO_2 + 2e^- \rightarrow Ti_3O_5 + O^{2-} \tag{1}$$

$$2Ti_3O_5 + 2e^- \rightarrow 3Ti_2O_3 + O^{2-} \tag{2}$$

$$CaTiO_3 + 2e^- \rightarrow Ca^{2+} + TiO + 2O^{2-} \tag{3}$$

$$Ti_2O_3 + 2e^- \rightarrow 2TiO + O^{2-} \tag{4}$$

$$TiO + 2e^- \rightarrow 2TiO + O^{2-} \tag{5}$$

$$TiO_2 + Ca^{2+} + O^{2-} \rightarrow CaTiO_3 \tag{6}$$

The reduction behaviour of TiO_2 pellets, thin-films and metal-cavity electrodes can be rationalised by reference to an electrochemical predominance diagram (EPD) [6], Figure 2. Here, electrode potential is shown vs. the negative logarithm of the oxide activity in the salt (pO^{2-}) and the thermodynamically stable species are indicated at different potential/oxide activity combinations. The bottom left hand corner corresponds to highly negatively polarized cathodes with a high O^{2-} concentration. The oxide content of electrolyte after pre-electrolysis has been determined to be in the range of three to four pO^{2-} [7].
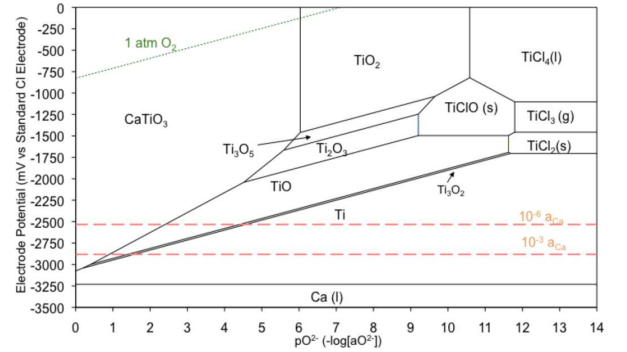
FIG. 1: Electrochemical predominance diagram for the system Ca-Ti-O-Cl at 1173 K.

The EPD (Figure 1) shows that the evolution of phases at a particular electrode potential is greatly dependent on the oxide content of the surrounding electrolyte. For example, reducing TiO_2 in oxide-saturated electrolyte ($pO^{2-} = 0$) will lead to a chemical reaction between CaO and TiO_2 to form $CaTiO_3$, which would subsequently reduce to titanium. If the electrolyte contained lower levels of oxide ($pO^{2-} = 6$), then TiO_2 would reduce through the lower titanium oxides to titanium. Thus it can be seen that the evolution of phases is dependent on several factors. Thus to achieve a consistent product the fundamentals of the process must be understood.

In all the aforementioned studies the phase identification is carried out ex-situ, once the samples have been cooled and

washed. This information is then correlated to *in-situ* voltammetric or amperometric data. However, upon cooling any number of phase and crystallographic changes or comproportionation and disproportionation reactions may take place. In addition, washing may remove water-soluble species. This has resulted in erroneous and conflicting reduction pathways being proposed. By performing *in-situ* synchrotron X-ray diffraction (SXRD) on a FFC Cambridge cell whilst reducing a pellet of TiO_2, we are able to present the first unequivocal description of the reduction pathway for TiO_2.

II. RESULTS

The scans for the gauge volume closest to the bottom surface (1.2 mm) of the sample are shown in Figure 2. The Rietveld refinements at key intervals in the reduction process are shown in Supplementary Figure 6. In some cases, due to the small gauge volume, insufficient grains were sampled to produce a true powder pattern. In these case there was some disparity between the observed and calculated peak intensities. By analysing the scans from the bottom side of the sample (0, 0.3, 0.6, 0.9 and 1.2 mm), molar fractions of the phases present were obtained (Figure 3).
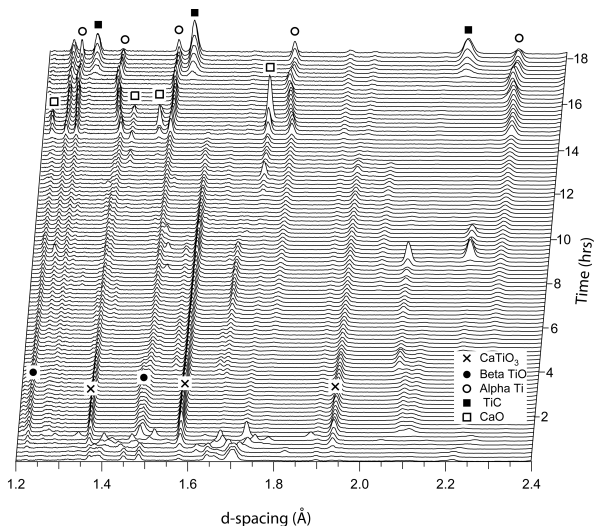

FIG. 2: Evolution of the diffraction patterns obtained near the surface of the pellet (1.2 mm from the centre).

The refined lattice parameters can be used to estimate the interstitial oxygen content in the α-Ti phase. The thermal expansion data for lattice parameter of Berry and Raynor [9], based on a temperature range of room temperature to 700°C, was combined with the room temperature dependence of oxygen content on lattice parameter measured by David *et al.* [8]. The data used are shown in Table I and the combined thermal and compositional effects are given in equations 7 and 8. It should be noted that the hexagonal *a*-axis length is largely independent of O content, so only the *c*-axis data was used in the analysis. It is further assumed that the titanium that first forms
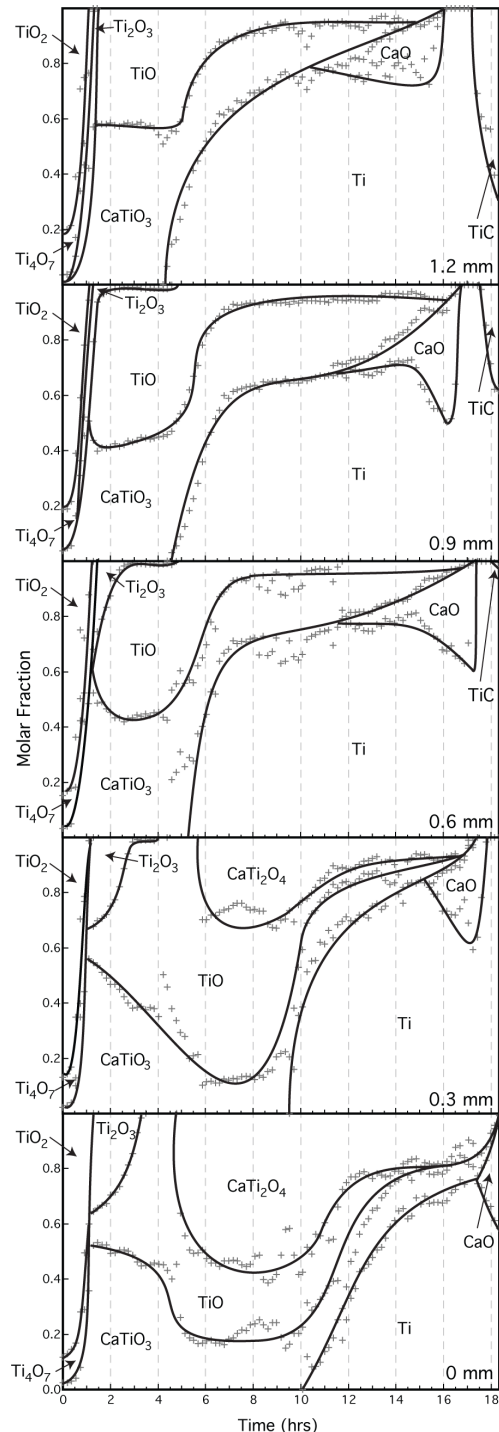
FIG. 3: Evolution of the phases present throughout the sample, obtained by Rietveld refinement.

was saturated with oxygen (14 wt.% O at 900°C). The variation in *c*-axis lattice parameter and inferred interstitial oxygen content in the α-Ti phase are shown in Figure 4. By combining this data with the phase fraction information the total oxygen content at different locations have been estimated, along with the total pellet oxygen content for comparison with the

TABLE I: α-Ti single crystal thermal expansion coefficients and dependence of lattice parameter on oxygen content - C(O).

a_0 (nm)*	0.29511 [11]
c_0 (nm)*	0.46826 [11]
$\alpha_a \times 10^{-6}$ (K^{-1})	11.03 [10]
$\alpha_c \times 10^{-6}$ (K^{-1})	13.37 [10]
da/dC(O) $\times 10^{-4}$ (nm at. %$^{-1}$)	0.78459 [11]
dc/dC(O) $\times 10^{-4}$ (nm at. %$^{-1}$)	4.7112 [11]

* Measured at room temperature, ∼ 0 ppm oxygen
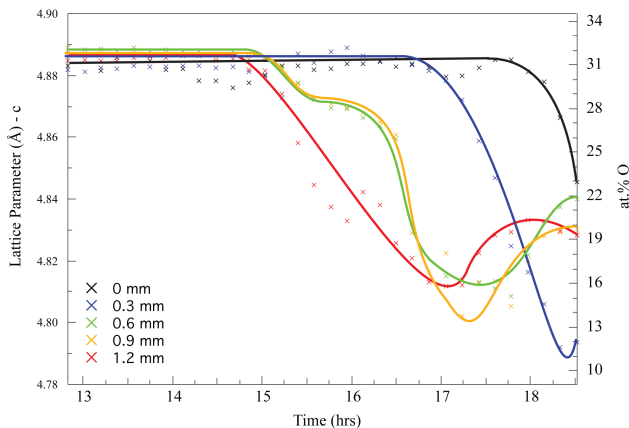
time-current data, Figure 5.

FIG. 4: Variation in the c - lattice parameter of α-Ti and inferred interstitial oxygen content during reduction.

$$a_{\alpha\text{Ti}} = a_0(1 + \Delta T \alpha_\alpha) + C(O)\frac{da}{dC(O)} \quad (7)$$

$$c_{\alpha\text{Ti}} = c_0(1 + \Delta T \alpha_\alpha) + C(O)\frac{dc}{dC(O)} \quad (8)$$

The first scans of the gauge volumes (Figure 3) reveals that rutile (TiO$_2$), Ti$_4$O$_7$ and CaTiO$_3$ are present at the beginning of reduction. The presence of Ti$_4$O$_7$ is consistent with the general electronic theory of TiO$_2$ [10–12], which states that when TiO$_2$ is subjected to a low oxygen atmosphere it begins to equilibrate with the atmosphere. This is achieved via the creation of defects in the crystal structure, which results in TiO$_2$ being reduced. It should be noted that in addition to Ti$_4$O$_7$, other Magnèli phases (e.g Ti$_5$O$_9$) fit relatively well, indicating that a range of Magnèli phases is present with the main phase being Ti$_4$O$_7$. This is the Magnèli phase most often detected during the FFC reduction of TiO$_2$ systems [3, 13].

The transformation to substoichiometric TiO$_2$ phases and subsequent release of oxygen ions into the electrolyte, results in the formation of CaTiO$_3$. This is supported by the work of Jiang *et al.* [14], whom suggest that the slight reduction of TiO$_2$ facilitates the transformation to the perovskite structure
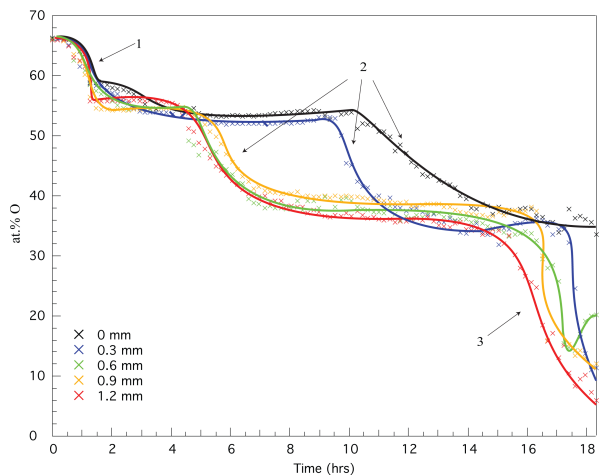

FIG. 5: Evolution of oxygen content at different locations in the pellet (a) and total oxygen content of the pellet compared to the current variation during reduction (b).

of CaTiO$_3$.

It is interesting to note that the phase Ti$_3$O$_5$ is not detected during reduction. Both the Ti-O phase diagram [15] and the EPD (Figure 1) predict that this phase should precede the formation of Ti$_2$O$_3$. In addition, significant quantities were observed by Schwandt *et al.* [3], by Dring *et al.* [5] and by the authors during *ex-situ* analysis of thin films. The narrow homogeneity range of Ti$_3$O$_5$ as shown in the EPD (Figure 1 and Ti-O phase diagrams indicates that significant quantities would only form *in-situ* if the electrode potential were held within the Ti$_3$O$_5$ phase field. It is hypothesised that the significant quantities of Ti$_3$O$_5$ observed by Schwandt *et al.* were a result of a disproportionation reaction of Magnli phases during cooling. It can be concluded that either the Ti$_3$O$_5$ field of stability is traversed rapidly or that kinetic considerations prevent it from forming during reduction. Thus the observed formation of Ti$_3$O$_5$, by the aforementioned authors, would be a result of a disproportionation reaction during the cooling of Magnéi phases.

Ti$_2$O$_3$ seems to have a more significant impact on reduction at the reduction temperature. It is detected at each gauge volume. Figure 8 shows that Ti$_2$O$_3$ reduces to cubic TiO. The monoclinic variant, alpha TiO, and Ti$_3$O$_2$, are not detected despite the fact that the Ti-O phase diagram [15] would suggest that they would form at temperatures less than 940 °C. The beta TiO then gradually reduces to alpha Ti.

CaTiO$_3$ and, in the inner regions of the pellet, CaTi$_2$O$_4$, are present for all but the last few hours of the reduction process. CaTiO$_3$ is reported to have a large compositional range [17], however the derived lattice parameters for CaTiO$_3$ remain quite consistent throughout reduction range. The authors have previously speculated that CaTiO$_3$ can to some degree act as a solid electrolyte allowing the transmission of oxide ions [7]. This could possibly account for the consistent stoichiometry of CaTiO$_3$. At the surface layers it would appear that CaTiO$_3$ is reduced directly to Ti despite the fact that thermodynam-

ically this would only occur at very low pO_{2-}. In the inner layers $CaTi_2O_4$ forms at the expense of $CaTiO_3$ and TiO. $CaTi_2O_4$ has previously been detected by the authors [17] and Schwandt et al. [3] in pellet reductions of TiO_2 based systems. It was theorised that the formation of this phase was either a result of the electrochemical reduction of $CaTiO_3$ or the result of a comproportionation reaction between $CaTiO_3$ and TiO. Figure 3 clearly shows that the formation of this phase clearly results in the equimolar consumption of TiO and $CaTiO_3$ indicating that a comproportionation reaction is indeed responsible for its formation (reaction 9).

$$CaTiO_3 + TiO \rightarrow CaTi_2O_4 \qquad (9)$$

The conditions required to form $CaTi_2O_4$ have been studied by Rogge et al. [18]. $CaTiO_3$ and titanium metal powder were combined with a $CaCl_2$ flux at $1000\,^{\circ}C$ to form $CaTi_2O_4$. It was shown that equimolar or titanium rich mixtures were needed to form the compound. Rogge et al. [18] also observed that when the titanium powder oxidised to TiO, $CaTi_2O_4$ was not formed, indicating that the comproportionation reaction probably has a small positive ΔG. Figure 3 shows that the formation of $CaTi_2O_4$ at the inner layers closely coincides with the formation of titanium in the outer layers (0.6, -0.9 and 1.2 mm). Formation of titanium in the outer layers will improve the electrical conductivity of those layers, in effect, making them an extension of the titanium current collector. This would improve the electrochemical reducing conditions in these layers allowing mixtures of TiO and $CaTiO_3$ to comproportionate.

Figure 5 shows that significant removal of oxygen takes place at events 1, 2 and 3. When correlated to the molar fractions charts (Figure 3), event 1 can be identified as the formation of TiO. For the surface layers (1.2, -0.9 and 0.6 mm), event 2 was identified as the reduction of TiO to titanium. For the inner layers (0.3 and 0 mm) event 2 is retarded due to the formation of $CaTi_2O_4$. Event 3 relates to the removal of CaO, which occurs at all locations with the exception of the centre (0 mm). Following the dissolution of CaO, the removal of interstitial oxygen from titanium commences.

CaO is detected throughout the pellet at the later stages of reduction. This phase forms when the electrolyte in the pores becomes saturated with oxide ions (22 mol.%). The onset of CaO formation appears to correlate with the reduction of $CaTi_2O_4$ in the inner layers. This results in a rapid evolution of oxide ions that have to be transported through the pellet pores to the bulk electrolyte. During reduction the porosity of the pellet, which is originally highly porous (60% open porosity), is reduced through a combination of sintering of titanium and formation of titanate phases. This significantly reduces the permeability of the pellet allowing oxide ion saturation to occur. Once event 2 is complete at the inner layers the flux of oxide ions passing through the pellet diminishes. At this point the surface CaO rapidly dissolves which is closely followed by the subsequent inner layers.

The formation of TiC is another important event. This phase is often seen as a surface layer in reduced pellets. Two mechanisms for TiC formation have been put forward by the authors [7]. The first suggests that TiC is formed as a result of a chemical reaction with carbon dust floating on the surface of the electrolyte that occurs as the sample is removed from the electrolyte. However the data supports the second mechanism, which involves the electrochemical deposition of carbon and subsequent reaction at the cathodic titanium surface of the pellet. This occurs via the chemical formation of CO_3^{2-} via a reaction between CO_2 formed at the anode and O^{2-} in the electrolyte (reaction 10). This complex then is reduced at the cathode to form CaO and carbon. The carbon then chemically reacts with alpha titanium to form TiC (reaction 11).

$$CO_2 + O^{2-} \rightarrow CO_3^{2-} \qquad (10)$$

$$CO_3^{2-} + Ti + 4e^- \rightarrow 3O^{2-} + TiC \qquad (11)$$
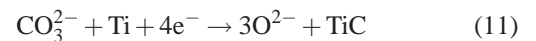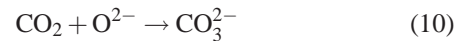
TiC formation is restricted to the surface of the pellet and only forms at the later stages of the process. It is proposed that TiC only forms once the cathode is sufficiently negatively polarised for reaction 11 to take place. The potential at which this takes place will be dependant on the activity of both the carbonate and oxide ions with the oxide ion activity having the dominant role. The oxide ion concentration in the region of the pellet will only reduce once reduction is nearly complete. Thus reaction 11 becomes more favourable once the process nears completion. Another interesting effect related to TiC is that an increase in lattice parameter c (Figure 4 was observed at the later stages of reduction at gauge volumes 0.6, 0.9 1.2 mm. This increase coincides with the formation of TiC. As TiC is a low oxygen phase when compared with alpha Ti the formation of TiC would causes the oxygen to partition into the alpha titanium, leading to an increase in oxygen content and lattice parameter c. In addition carbon has limited solubility in alpha titanium (0.15 at. %), which could result in an increase in lattice parameter. The low solubility of oxygen in TiC could retard the formation of TiC until the oxygen content in the titanium is sufficiently low.

III. DISCUSSION

The key findings of this paper can be summarised as follows. It was found that upon entering the low oxygen atmosphere, within the apparatus, TiO_2 quickly forms substoichiometric phases, which significantly improves ionic conductivity over stoichiometric TiO_2. In contradiction to the work of Schwandt et al. [3], it was found that $CaTiO_3$ forms chemically from the substoichiometric TiO_2 phases. $CaTi_2O_4$ was found to form from the comproportionation of TiO and $CaTiO_3$ and was detrimental to the reduction process. The phases Ti_3O_5, alpha TiO and Ti_3O_2 were not observed despite being predicted by the Ti-O phase diagram. The formation and eventual dissolution of CaO was related to the oxide flux within the pellet. The deoxidation of titanium was found to occur only once CaO had been removed locally within the

pellet. TiC was determined to form on the reduced pellet surface through an *in-situ* electrochemical process but only occurred when the oxygen content in the titanium reached approximately 16 at. %.

The relative ease by which low electrical conductivity TiO_2 can be reduced via the FFC Cambridge process can be attributed to the low O_2 partial pressure in the apparatus. This results in a nearly instantaneous formation of electrically conductive Magnèli phases. The time required to reduce TiO_2 pellets appears to be controlled by the formation of calcium compounds ($CaTiO_3$, $CaTi_2O_4$ and CaO). Their formation causes reduces the permeability of the pores effectively causing passivation. As a result understanding the mechanism by which these phases form and, more importantly, how to prevent their formation is key to improving the efficiency of the process. The chemical formation of $CaTiO_3$, and hence the subsequent formation of $CaTi_2O_4$ could be avoided if metal oxides with lower valence titanium oxides (i.e. Ti_2O_3 and TiO) are used as a starting product. Preventing the formation of the titanates will improve permeability and hence decrease the likelihood of oxide saturation and hence CaO formation. Alternatively engineering of the preform geometry to maximise initial pore size and permeability could reduce the deleterious effect of titanate formation. The formation of titanium carbide appears to be unavoidable with the current cell design. Its formation can only be prevented if carbon free anodes are employed or a membrane is used.

IV. METHODS

To form the TiO_2 precursors, reagent grade TiO_2 (99.5% Alfa Aesar) was ball milled with ethanol and zirconia spheres for 24 h. The slurry was dried and the powder ground in a mortar and pestle with a small quantity of distilled water, which acted as a binding agent. 0.4 g of powder was placed into a 13 mm diameter die prior to uniaxial compaction at 100 MPa. The precursors were then drilled to accept the commercial purity Ti cathodic current collector and placed in an alumina-firing trough and sintered in argon (BOC pureshield - 150 mLmin^{-1} at 1373 K for 3h at a rate of 3 Kmin^{-1}. The pellets were then ground to reduce the pellet diameter and weight to approximately 7 mm and 0.2 g respectively.

The electrochemical cell was designed to minimise attenuation of the white X-ray beam and avoid additional sources of diffraction. Reductions were performed in a resistance furnace-heated quartz glass reaction vessel (Figure 7), based on that used previously [20]. Openings were incorporated into the furnace to allow the synchrotron X-ray beams to pass. A glassy carbon crucible was used to contain the salt and act as a consumable anode. Calcium chloride granules (Fluka) were dried and prepared [20] within the carbon crucibles which were then vacuum sealed prior to use.

The apparatus was heated at a rate of 1 Kmin^{-1} under argon (BOC pureshield - 50 mLmin^{-1}) from room temperature to the electrolysis temperature (1173 K). The electrolyte was then thermally equilibrated for three hours. Prior to experiments the salt was pre-electrolysed for $1-3$h to remove electro-active impurities by polarising a grade 2 CP-Ti rod (3 mm) versus the graphite crucible.

The sintered metal oxide precursor was attached to the titanium current collector and suspended above the salt prior to pre-electrolysis. Following the pre-electrolysis the precursor was lowered into the molten salt and polarised at a rate of 0.5 mVs^{-1} from open circuit to -3100 mV versus the carbon anode.

The ID15A beamline at the ESRF was used to produce an unmonochromated (white) X-ray beam in an energy dispersive mode. A 50 µm by100 µm incident beam and $5°$ scattering angle were defined by slits yielding a gauge length of 1000 µm (Supplementary Figure 7). The assembly was mounted on a translation stage allowing nine locations at different heights in the pellet to be studied. Diffraction spectra were collected for 6 s each for a total reduction time of 67 ks (18.5 h).

The SXRD plots produced for each time and position were analyzed by Rietveld refinement using GSAS [20], allowing the phases present to be identified and atomic fractions to be obtained. The source spectrum was normalized using both an Al powder and the powder TiO_2 pattern obtained from the pellet prior to insertion into the cell. Beam hardening within the cell was accounted for by comparison with the initial patterns obtained from the pellet.

[1] Chen G., Fray D.J. and Farthing T.W., Direct Electrochemical Reduction of Titanium Dioxide in Molten Calcium Chloride. Nature, 2000. 407: p. 361-364.

[2] Kroll W., The Production of Ductile Titanium. Seventy-Eighth General Meeting, 1940: p. 35-47.

[3] Schwandt C. and Fray D.J., Determination of the kinetic pathway in the electrochemical reduction of titanium dioxide in molten calcium chloride. Electrochimica Acta, 2005. 51(1): p. 66-76.

[4] Rao K., Brett D., Inman D. and Dashwood R.J., Investigation of the Reduction Electrochemistry of Titanium Oxides in Molten Calcium Chloride Using Cavity Electrode. in Ti-2007. 2007. Japan: The Japanese Institute of Metals.

[5] Dring K., Dashwood R.J. and Inman D., Voltammetry of Tita-

nium Dioxide in Molten Calcium Chloride at 900°C. Journal of The Electrochemical Society, 2005. 152(3): p. E104-E113.

[6] Dring K., Dashwood R.J. and Inman D., Predominance Diagrams for Electrochemical Reduction of Titanium Oxides in Molten CaCl$_2$. Journal of The Electrochemical Society, 2005. 152(10): D184-D190.

[7] Bhagat R., The Electrochemical Formation of Titanium Alloys Via the FFC Cambridge Process, in Departemnt of Materials. 2008, Imperial College London: London. p. 1-133.

[8] David D., Garcia E.A., Lucas X. and Beranger G., Etude de la Diffusion de l'Oxygene Dans le Titane a Oxyde Entre 700°C et 950°C Journal of the Less-Common Metals, 1979. 65: p. 51-69.

[9] Berry R.L.P. and Raynor G.V., Research, 1953. 6(21S).

[10] Bak T., Nowotny J., Rekas M. and Sorrell C.C., Defect Chem-

istry and Semiconducting Properties of Titanium Dioxide: II. Defect Diagrams. Journal of Physics and Chemistry of Solids, 2003. 64(7): p. 1057-1067.

[11] Nowotny J., Radecka M. and Rekas M., Semiconducting Properties of Undoped TiO_2 Journal of Physics and Chemistry of Solids, 1997. 58(6): p. 927-937.

[12] Nowotny J., Radecka M. and Rekas M., Sugihara S., Vance E.R. and Weppner W., Electronic and Ionic Conductivity of TiO_2 Single Crystal Within the n-p Transition Range. Ceramics International, 1998. 24(8): p. 571-577.

[13] Alexander D.T.L., Schwandt C. and Fray D.J., Microstructural Kinetics of Phase Transformations During Electrochemical Reduction of Titanium Dioxide in Molten Calcium Chloride. Acta Materialia, 2006. 54(11): p. 2933-2944.

[14] Jiang K., Hu X., Ma M., Wang D., Qiu G., Jin X. and Chen G.Z., "Perovskitization" - Assisted Electrochemical Reduction of Solid TiO_2 in Molten $CaCl_2$. Angewandte Chemie International Edition, 2006. 45(3): p. 428-432.

[15] Murray J.L. and Wriedt H.A., O-Ti Phase Diagram. ASM International. 1987, Ohio. 148-165.

[16] Bak T, Nowotny J and Sorrel CC, Chemical Diffusion in Calcium Titanate. Journal of Physics and Chemistry of Solids, 2004. 65(7): p. 1229-1241.

[17] Bhagat R., Jackson M., Inman D. and Dashwood R.J., Production of Ti–W Alloys from Mixed Oxide Precursors via the FFC Cambridge Process. Journal of The Electrochemical Society, 2009. 156(1): p. E1-E7.

[18] Rogge M.P., Caldwell J.H., Ingram D.R., Green C.E., Geselbracht M.J. and Siegrist T., A New Synthetic Route to Pseudo-Brookite-Type $CaTi_2O_4$. Journal of Solid State Chemistry, 1998. 141: p. 338-342.

[19] Bhagat R., The Electrochemical Formation of Titanium Alloys Via the FFC Cambridge Process, in Departemnt of Materials. 2005, Imperial College.

[20] Larson A.C. and Von Dreele R.B., Los Alamos National Laboratory Report, 2000. LAUR(86).

V. AUTHORS CONTRIBUTION

R. J. Dashwood and D. Dye conceived and designed the study. B. K. Jackson, R. J. Dashwood and D. Dye designed the apparatus, which B. K. Jackson built and commissioned the apparatus. R. Bhagat, R. J. Dashwood, D. Dye, S. L. Raghunathan, R.J. Talling, K. K. Rao and conducted the experiments. R. Bhagat and S.L. Raghunathan analysed the data with support from R.J. Talling, R. J. Dashwood and D. Dye. The paper was written by R. Bhagat with contributions and editing from R. J. Dashwood, D. Dye, D. Inman, R.J. Talling and S.L. Raghunathan.
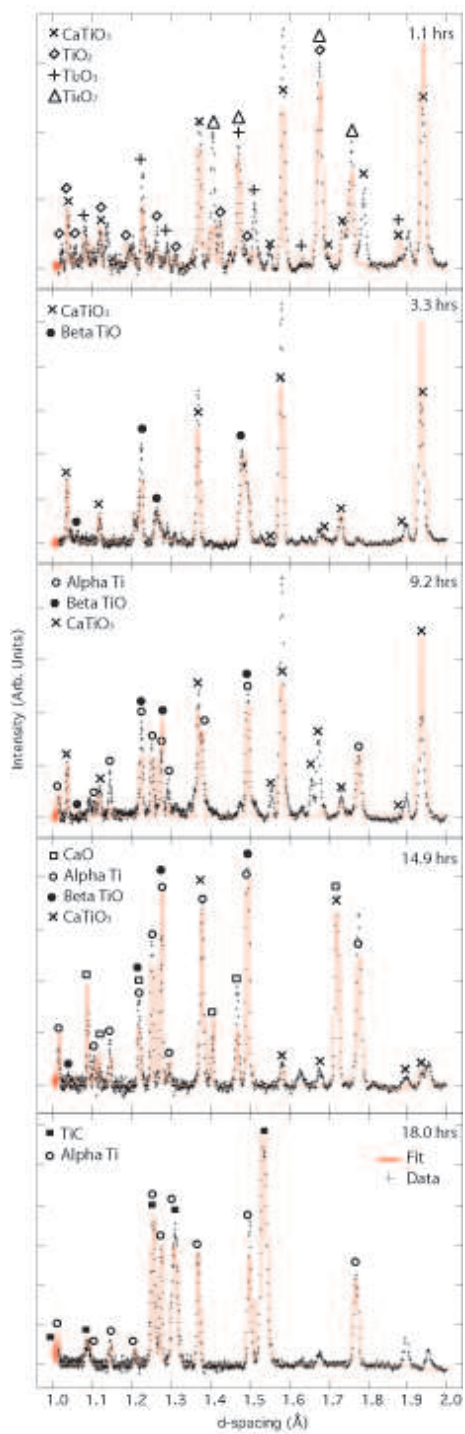
VI. SUPPLEMENTARY FIGURES

FIG. 6: Rietveld refinements and diffraction spectra obtained near the surface of the pellet (1.2 mm from the centre). Key peaks labelled.
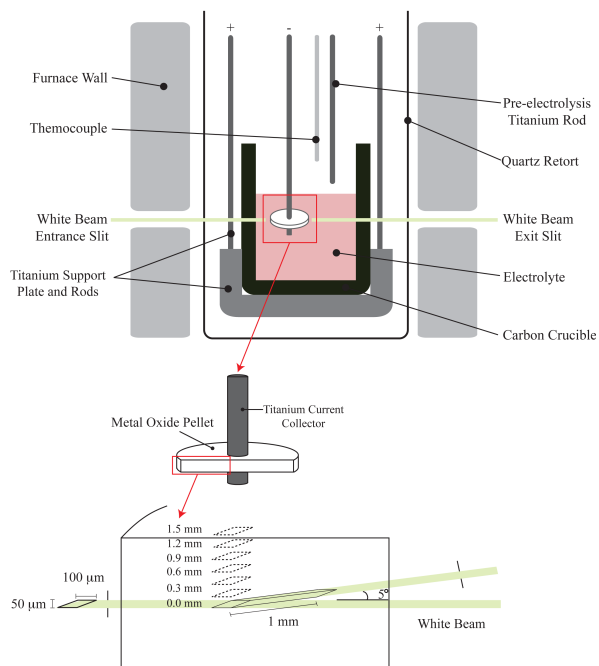
FIG. 7: Schematic of electrochemical apparatus used for the in situ X-ray studies, showing several gauge volumes present during experimentation.